Mon. Not. R. Astron. Soc. **000**, 1–?? (2012) Printed 3 April 2013 (MN LATEX style file v2.2)

Effects of superstructure environment on galaxy groups

H. E. Luparello[1], M. Lares[1], C.Y. Yaryura[1], D. Paz[1], N. Padilla[2,3] and D. G. Lambas[1]
[1]*Instituto de Astronomía Teórica y Experimental (CONICET-UNC). Observatorio Astronómico de Córdoba, Laprida 854, X5000BGR, Córdoba, Argentina*
[2]*Departamento de Astronomía y Astrofísica, Pontificia Universidad Católica de Chile, Santiago, Chile*
[3]*Centro de Astro-Ingeniería, Pontificia Universidad Católica de Chile, Santiago, Chile*

Released 2012 Xxxxx XX

ABSTRACT
We analyse properties of galaxy groups and their dependence on the large-scale environment as defined by superstructures. We find that group–galaxy cross–correlations depend only on group properties regardless the groups reside in superstructures. This indicates that the total galaxy density profile around groups is independent of the global environment. At a given global luminosity, a proxy to group total mass, groups have a larger stellar mass content by a factor 1.3, a relative excess independent of the group luminosity. Groups in superstructures have 40 per cent higher velocity dispersions and systematically larger minimal enclosing radii. We also find that the stellar population of galaxies in groups in superstructures is systematically older as infered from the galaxy spectra Dn_{4000} parameter. Although the galaxy number density profile of groups is independent of environment, the star–formation rate and stellar mass profile of the groups residing in superstructures differs from groups elsewhere. For groups residing in superstructures, the combination of a larger stellar mass content and star–formation rate produces a larger time–scale for star formation regardless the distance to the group center. Our results provide evidence that groups in superstructures formed earlier than elsewhere, as expected in the assembly bias scenario.

Key words: large scale structure of the universe - statistics - data analysis

1 INTRODUCTION

The large–scale structure of the Universe appears as a network made up of walls, filaments, knots and voids (Joeveer et al. 1978; Gregory & Thompson 1978; Zeldovich et al. 1982; de Lapparent et al. 1986). The nodes are the intersections of walls and filaments, so they are the highest density regions, usually known as superclusters. Supercluster of galaxies are the largest systems present in the Universe. There are many galaxy groups and clusters inhabiting these large systems. Studies of the galaxy clusters according to their environment are useful to understand the properties and evolution of both, galaxy clusters themselves and the large–scale structure of the Universe. Besides, studying their influence on galaxy clusters it is possible to analyse properties and the evolution of large–scale structure. Recent galaxy redshift surveys (e.g. York et al. (2000); Colless et al. (2001)) sample a sufficiently large volume to allow the study of the influence of supercluster in galaxy groups. There are many previous studies, both theoretical and observational, that show that richer and more luminous groups and clusters of galaxies are located in higher density environments (Einasto et al. 2003, 2005; Croft et al. 2012); while the galaxy properties, such as the star–formation rate or galaxy colours, also depend on large–scale structure (Binggeli 1982; Donoso et al. 2006; Crain et al. 2009; White et al. 2010). Einasto et al. (2007) analised the properties of galaxies in superclusters in the 2dFRS galaxy catalogue, and found that galaxy morphologies and their star formation activity are influenced by both the local and global environments. Park & Choi (2009) used a volume–limited sample of galaxies extracted from the SDSS–DR4 to show that the influence of the large–scale density is not very significant over several galaxy properties once luminosity and morphology are fixed. However they suggest that this weak residual effect is due to the dependence of halo gas property on the large–scale density. Regarding to numerical simulations, Gil-Marín et al. (2011) took into account the environmental influence proposing an extension of the halo model. The formation and evolution of systems that are embedded in superstructures could be conditioned by these large overdensities (Hoffman et al. 2007; Araya-Melo et al. 2009; Bond et al. 2010; Pompei & Iovino 2012, and references therein). In high density regions clusters have a larger amount of substructures and higher peculiar velocities of their main galaxies than in low density regions (Einasto et al. 2005; Tempel et al. 2009).

Most recent results are presented in Einasto et al. (2012); Lietzen et al. (2012) and Costa-Duarte et al. (2012). Distinguishing between spider and filamentary morphology of superclusters, Einasto et al. (2012) found that clusters in spider shape superclusters tend to have more substructure and higher peculiar velocities than cluster in filamentary superclusters. Furthermore, clusters that are not members of superclusters have less substructure and lower values of peculiar velocities than supercluster members (Einasto et al. 2012). Costa-Duarte et al. (2012) verified the results found by Einasto et al. (2012) and also studied the effect of environment on galaxies in clusters and their outskirts. They suggest that the stellar

population of clusters does not depend on supercluster richness nor morphology. Lietzen et al. (2012) studied how the galaxy evolution is influenced by the local group scale and the large scale environment. They found that in voids, the fraction of passive and star–forming galaxies in groups are approximately equal, while in superclusters the fraction of passive galaxies are considerably larger than those of star–forming galaxies. Moreover, equally rich groups are more luminous in superclusters than in voids. In this work, we will analyse the properties of galaxy groups located in large superclusters.

This paper is organized as follows. In Section 2 we present the data samples extracted from the galaxy, group and supercluster catalogues. In Section 3 we show the results of the analysis of group properties and their dependence with the large scale environment characterized by superstructures. Discussion and conclusions and given in Section 4. Throughout this paper, we adopt a concordance cosmological model ($\Omega_\Lambda = 0.75$, $\Omega_{matter} = 0.25$) in the calculation of distances.

2 DATA AND SAMPLES

2.1 SDSS–DR7

One of the largest and most ambitious surveys carried out so far is the Sloan Digital Sky Survey (York et al. 2000). It has deep multicolor images covering more than one quarter of the sky and creates three-dimensional maps containing more than 930000 galaxies and more than 120000 quasars. Its main goal is the study of large-scale structure of the Universe, producing also astronomical data for other areas. In particular, in this work we use the Seventh Data Release (DR7) of the spectroscopic galaxy catalogue. It is one of the largest data sets produced by this project and contains images, image catalogues, spectra and redshifts. The limiting magnitude of the spectroscopic galaxy catalogue in the r–band is $m_r = 17.77$ (Strauss et al. 2002). The information about this survey is publicly available [1]. We also use the MPA-JHU DR7 (Kauffmann et al. 2003), which provides additional information about star–formation rates, stellar masses and the spectral indicator Dn_{4000}. The star–formation rates (SFRs) are computed following the procedure described by Brinchmann et al. (2004).

Regarding to the stellar masses, they are obtained as explained in Kauffmann et al. (2003) and Salim et al. (2007). Spectral indicators are usually computed to quantify spectral evolution of galaxies. A widely used parameter is the Dn_{4000} index, introduced by Hamilton (1985). The 4000Å break amplitude is obtained from the ratio of the averaged flux density above 4000Å to the averaged flux density below 4000Å (Hamilton 1985). The ranges used to compute that averages are 4050 – 4250Å and 3750 – 3950Å. The break at 4000Å is produced by the absorption of metalic lines, specially Fraunhofer H and K lines of CaII, and lines of various elements heavier than Helium in several stages of ionization. The opacity for photons bluer than $\lambda \sim 4000$Å rapidly increases, producing a characteristic change in the intensity. This intensity drop is enhanced in galaxies with metal rich, old stellar populations. Also, the Balmer lines close to 4000Å become broader and deeper with time from the starburst (Sánchez Almeida et al. 2012). This parameter is a good indicator of stellar evolution, since it correlates with effective temperature, surface gravity and metalicity in stellar spectra (Gorgas et al. 1998, 1999).

[1] http://www.sdss.org/dr7

2.2 Catalogue of Superstructures

The clustering properties of galaxies in scales smaller than the size of superstructures are key to observationally constrain the accretion process that give rise to luminous galaxies. The evolution of the supercluster–void network depends on the matter/energy contents of the universe, and thus are sensitive to the cosmological model. Using numerical simulations of a LCDM universe evolved up to a scale factor 100 times the present value, Dünner et al. (2006) find that there is a minimum mass overdensity for a structure to remain bound in the future. According to this, they stablish a criteria to identify structures in the present day universe that are likely to evolve into virialized structures. On the other hand, Einasto et al. (2007) proposed a method to identify superstructures from a smoothed luminosity density field. The authors build a superstructure catalogue by isolating large regions in space that have a luminosity above a given threshold, calibrated so that the largest superstructure is limited to the size of the largests known superclusters. The density field method can be combined with the results from numerical simulations to establish, assuming a constant mass to luminosity relation, criteria to isolate structures that are likely to evolve into virialized structures in the distant future Luparello et al. (2011). We use this catalogue of "superstructures", i.e., systems that are Future Virialized Structures (hereafter FVS) to characterize the large scale environment of galaxies. The catalogue of FVS was extracted from a volume-limited sample of galaxies from the SDSS–DR7, with a limiting absolute magnitude of $M_r < -20.47$, in the redshift range $0.04 < z < 0.12$. The luminosity-density field is constructed on 1 h^{-1} Mpc cubic cells grid, applying an Epanechnikov kernel of $r_0 = 8$ h^{-1} Mpc (equation 3 of Luparello et al. (2011)). The structures are constructed by linking overdense cells with a "Friends of Friends" algorithm, using a luminosity overdensity threshold of $D_T = \rho_{lum}/\bar{\rho}_{lum} = 5.5$. They also assign a lower limit for the total luminosity of a structure at $L_{struct} \geqslant 10^{12} L_\odot$ to avoid contamination from smaller systems. The main catalogue of superstructures has completeness over 90 per cent and contamination below 5 per cent, according to calibrations made using mock catalogues. The volume covered by the catalogue is 3.17×10^7 (h^{-1} Mpc)^3, within which 150 superstructures were identified, composed by a total of 11394 galaxies. FVS luminosites vary between 10^{12} $L_\odot$ and $\simeq 10^{14}$ $L_\odot$, and their volumes range between 10^2 (h^{-1} Mpc)^3 and 10^5 (h^{-1} Mpc)^3.

The authors analysed 3 samples of SDSS–DR7 galaxies with different luminosity thresholds, dubbed S1, S2 and S3, and are described in Table 1 of their paper. We will consider sample S2 in our analysis, which contains 89513 galaxies with $Mr < -20.47$ in the intermediate redshift range $0.04 < z < 0.12$.

2.3 Galaxy Group Samples

The galaxy groups used in this work are identified in the SDSS-DR7 galaxy catalogue following Zapata et al. (2009). The identification of these groups uses the same method presented in Merchan & Zandivarez (2005), who implemented a Friends of Friends (FoF) algorithm, with a variable projected linking length σ, with $\sigma_0 = 0.239 h^{-1} Mpc$ and a fixed radial linking length $\Delta v = 450 kms^{-1}$. These values were set by Merchan & Zandivarez (2005) to obtain a sample as complete as possible and with low contamination (95% and 8%, respectively). The variable linking lenght is calibrated to compensate the sample dilution with redshift, as the original sample of galaxies is flux-limited. The full catalogue comprises 17.106 groups, in the redshift range $0.001 < z < 0.5$. With

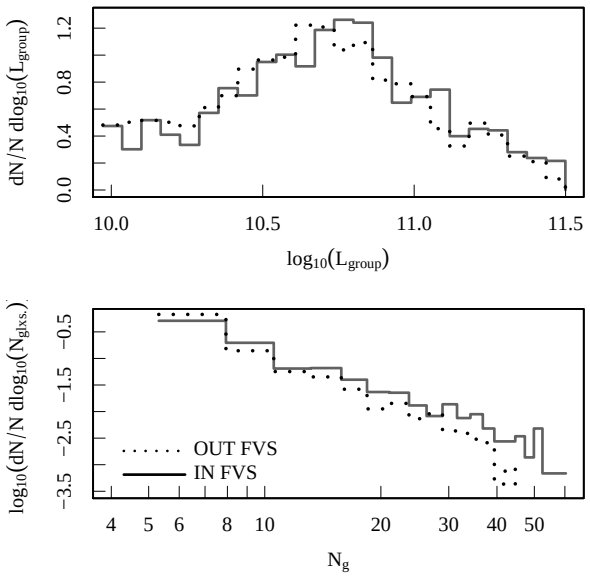

Figure 1. Luminosity (upper panel) and Multiplicity (bottom panel) distributions for the group samples inside (solid line) and outside (dotted line) superstructures.

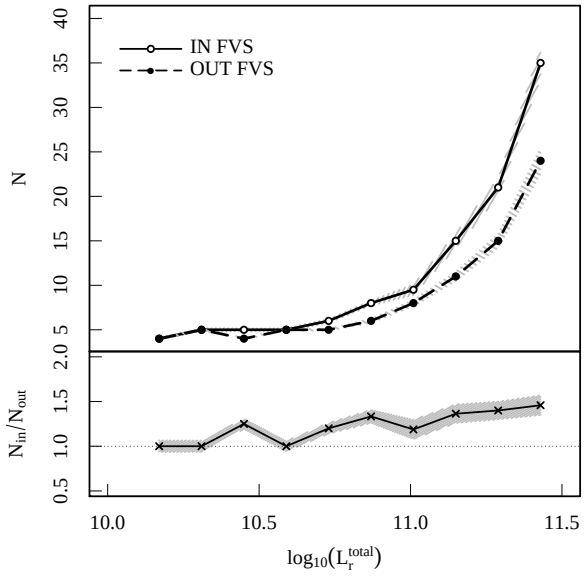

Figure 2. Upper panel: Mean multiplicity of groups, in bins of group mean luminosities, for groups in G_{in} (solid line) and G_{out} (dashed line). The error bands correspond to the error of the means. Bottom panel: ratio of multiplicity for group samples G_{in} and G_{out}.

the aim to study the influence of superstructures in the global properties of galaxy groups, we consider two subsamples of groups: those residing in FVS and those which are not members of FVS. It is well known that the luminosity correlates with the clustering amplitude (Alimi et al. 1988; Zehavi et al. 2005; Swanson et al. 2008; Wang et al. 2011; Zehavi et al. 2011; Ross et al. 2011). In order to avoid possible effects of total group luminosity (a suitable proxy to group total mass) we define samples in FVS and elsewhere, G_{in} and G_{out} respectively, by requiring them to have similar luminosity distributions. With this restriction, our group samples are suitable to study different properties of systems and their relation to environment. The resulting samples G_{in} and G_{out}, in the reshift range $0.06 < z < 0.12$, contain 1457 and 2645 groups, respectively, with the same luminosity distributions. All these groups comprise at least 4 galaxies brighter than $Mr < -20.47$, so that the final sample of galaxies in groups is volume limited up to $z = 0.12$. In the upper panel of figure 1 we show the luminosity distributions of samples G_{in} and G_{out} where it can be seen their similarity in the total luminosity range $10^{10} - 10^{11.5} L_{\odot}$.

Some studies have shown that properties of the galaxy groups correlate with the group multiplicity. Lietzen et al. (2012) found that the dependence of the fraction of different types of galaxies in groups varies with the richness of the group. These authors show that the fraction of star–forming galaxies declines and the fraction of passive galaxies increases as the richness of a group rises from one to approximately ten galaxies. They also show that the fraction of galaxies of different types do not depend on group richness, for groups comprising between 20 and 50 members. The lower panel of figure 1 shows the multiplicity distributions of the samples G_{in} and G_{out}. In order to analyse multiplicity dependence on system luminosity, we have computed the mean multiplicity in bins of total group luminosity. The results are shown in figure 2 where it can be seen that the number of galaxies in groups at a given total luminosity is larger in FVS by a factor 1.3.

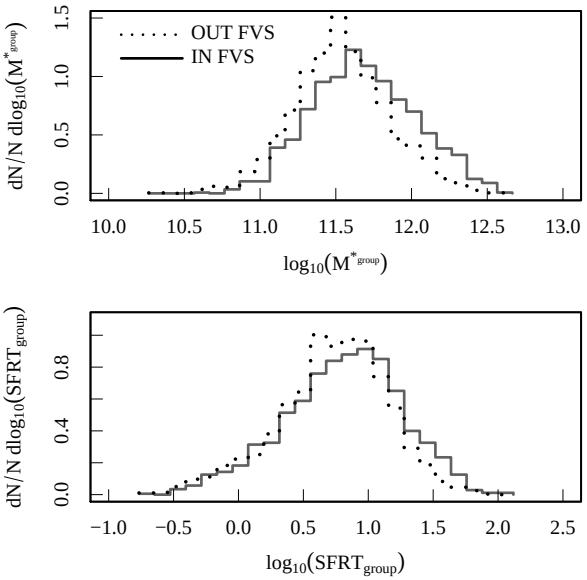

Figure 3. Stellar mass (upper panel) and total star–formation rate (bottom panel) distributions for the group samples inside (solid line) and outside (dotted line) superstructures.

3 PROPERTIES OF GALAXY GROUPS

3.1 Groups stellar mass, velocity dispersion and star formation time–scale

We have estimated the total stellar mass content of each group by adding the stellar masses of their members. In a similar fashion, we have also computed the total star–formation rate of the groups by adding the star–formation rates of the individual members. In figure 3 we show the resulting total group stellar mass (M^{*}_{group}) and to-

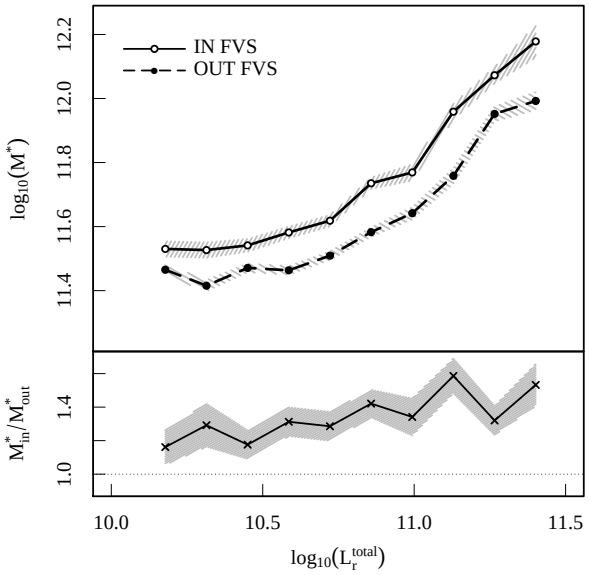

Figure 4. Upper panel: Mean total stellar mass of groups, in bins of group mean luminosities, for groups in G_{in} (solid line) and G_{out} (dashed line). The error bands correspond to the error of the means. Bottom panel: ratio of mean total stellar mass for group samples G_{in} and G_{out}.

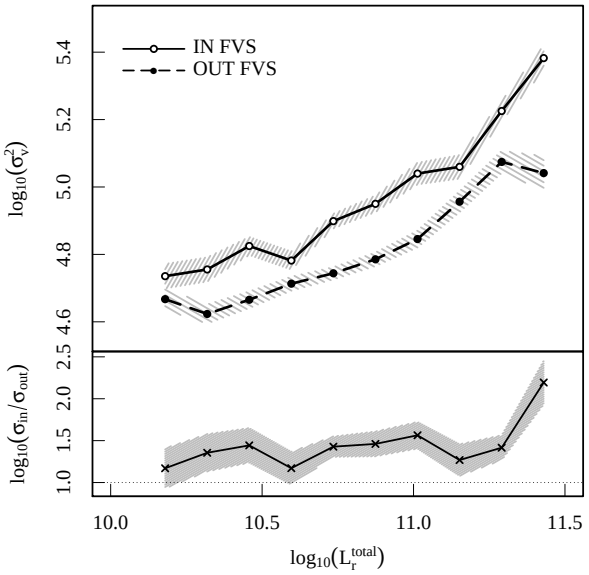

Figure 5. Upper panel: Mean velocity dispersions of groups, in bins of group mean luminosities, for groups in G_{in} (solid line) and G_{out} (dashed line). The error bands correspond to the error of the means. Bottom panel: ratio of mean velocity dispersions for group samples G_{in} and G_{out}.

tal group star–formation rate ($SFRT_{group}$) distributions for the two samples G_{in}, and G_{out}. It can be seen that the total stellar mass is systematically larger for groups residing in superstructures. Also, the total star–formation rate distributions shows this same tendency. The median total stellar mass content of groups in sample G_{in} is $4.6 \times 10^{11} M_{\odot}$, while the corresponding median in sample G_{out} is $3.4 \times 10^{11} M_{\odot}$. The star–formation rate medians are $6.7 M_{\odot} yr^{-1}$ and $5.7 M_{\odot} yr^{-1}$ for G_{in} and G_{out} group samples, respectively. We have also explored the difference of total stellar masses as a function of group luminosity. In Fig. 4 we show the mean total stellar mass as a function of group luminosity for G_{in} and G_{out} samples. By inspection to this figure, and in particular to the lower panel, it can be seen that the excess of the total stellar mass for groups residing in FVS is not strongly dependent on group luminosity. It should be noticed that the difference of the star–formation rate distributions is less significant than the difference of the stellar mass distributions (17 per cent excess in SFRT compared to 35 per cent in M* for sample G_{in}). These results have a natural explanation in a scenario where groups in FVS started their star–formation process earlier.

Velocity dispersion of groups can be used to explore the dynamics of these systems. We have also studied the dependence of the groups velocity dispersion on group luminosity for samples G_{in} and G_{out}. The results are given in Fig. 5, where it can be seen that groups located in FVS (sample G_{in}) present larger velocity dispersion than groups located in less dense environments, regardless of group luminosity. This results is consistent with Einasto et al. (2012) although we stress the fact that our samples G_{in} and G_{out} were selected to have groups with similar luminosity.

With the aim of assigning an indicator of the stellar time-scale at the present star–formation rate for groups we use a parameter defined as $\tau = M^*/SFRT$, analogous to the one defined for galaxies. Thus, τ provides an estimate of the time–scale for the formation of the total stellar mass of the group at the present rate of star formation. Figure 6 displays the results for groups of samples G_{in} and G_{out} showing a systematic trend for larger τ values for groups in

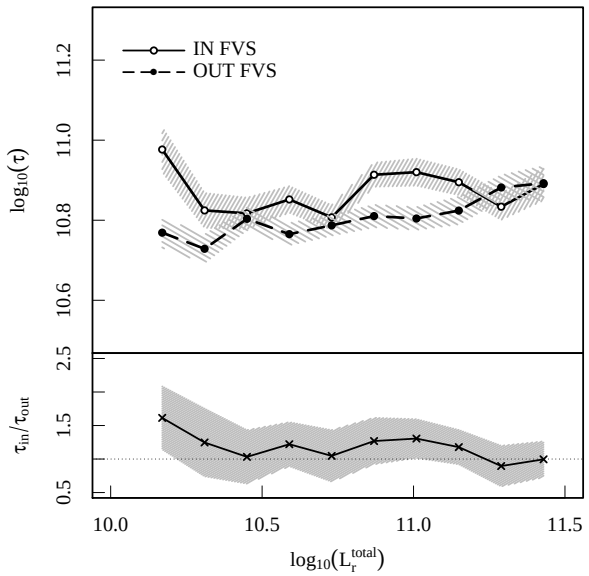

Figure 6. Upper panel: Mean stellar time–scale of groups, in bins of group mean luminosities, for groups in G_{in} (solid line) and G_{out} (dashed line). The error bands correspond to the error of the means. Bottom panel: ratio of stellar time–scale for group samples G_{in} and G_{out}.

FVS. It can also be seen that this tendency is larger at lower group luminosities.

We have computed the fraction of galaxies with spectra dominated by a young stellar population as revealed by the Dn_{4000} parameter. Figure 7 shows the mean values of F^{young}, such that $Dn_{4000} < 1.5$, for groups in samples G_{in} and G_{out}. As it can be seen, galaxies dominated by a young stellar population are more

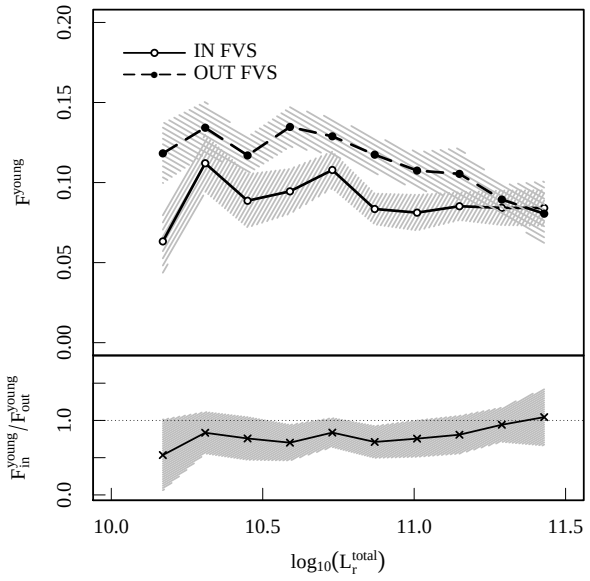

Figure 7. Fraction of young ($Dn_{4000} < 1.5$) galaxies in group samples G_{in} and G_{out} (F^{young}).The error bands correspond to the error of the means. Bottom panel: ratio of F^{young} for group samples G_{in} and G_{out}.

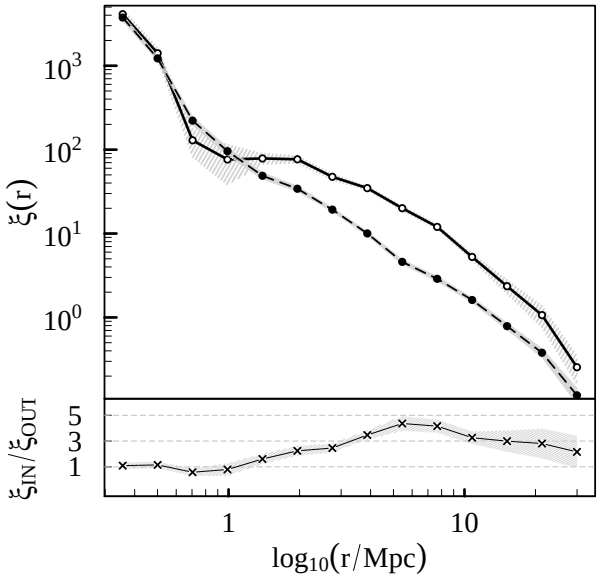

Figure 8. Group–galaxy cross–correlation functions for samples G_{in} (solid line) and G_{out} (dashed line), where the groups have the same total luminosity distributions. Shaded errors corresponds to Jacknife uncertanties.

frequently found in groups not belonging to superstructures. We also find that this effect is stronger at lower group luminosities.

3.2 Clustering properties

The aim of this section is to study the clustering of galaxies around group centres for G_{in} and G_{out} samples. For this purpose, we use two–point correlation statistics following the procedures described in Section 3 of Yaryura et al. (2012). The two–point galaxy–group cross–correlation function, $\xi(r)$, is defined as the excess of the probability of finding a galaxy, at a given distance from a group centre. Since we use redshift–space positions of galaxies, we estimate the correlation function ξ, as a function of the projected (σ) and line of sight (π) distances. Then, we implement the inversion method presented by Saunders et al. (1992) to obtain the spatial correlation function $\xi(r)$ from $\xi(\sigma, \pi)$. We integrate along the line of sight to obtain the projected correlation function $\Xi(\sigma)$:

$$\Xi(\sigma) = 2\int_0^\infty \xi(\sigma,\pi)d\pi = 2\int_0^\infty \xi(\sqrt{\sigma^2+y^2})dy. \quad (1)$$

We estimate the real space correlation function by the inversion of $\Xi(\sigma)$ assuming a step function $\Xi(\sigma_i) = \Xi_i$ in bins centered in σ_i and interpolating between $r = \sigma_i$ values (equation 26 of Saunders et al. 1992):

$$\xi(r) = -\frac{1}{\pi}\sum_{j\geqslant i}\frac{\Xi_{j+1}-\Xi_j}{\sigma_{j+1}-\sigma j} ln\left(\frac{\sigma_{j+1}+\sqrt{\sigma^2_{j+1}-\sigma^2_i}}{\sigma_j+\sqrt{\sigma^2_j-\sigma^2_i}}\right). \quad (2)$$

In terms of the halo model (Cooray & Sheth (2002) and references therein) all galaxies are associated with haloes, which are defined as dense objects that constitute the non–linear density field. In this context, the two–point correlation function can be interpreted as the sum of two types of galaxy pairs: pairs in the same halo (1–halo term), and pairs in separated haloes (2–halo term). On small scales ($r \lesssim 1Mpc$) the 1–halo terms dominates, while for larger scales it becomes negligible predominating the 2–halo term (Sheth 2005; Zehavi et al. 2004). We consider galaxies with r–band luminosities $M_r < -20.5$ and take the geometrical centres of groups as centres for the cross–correlation calculation. Figure 8 shows the resulting cross–correlation functions for group centres of samples G_{in} and G_{out}. The solid (dashed) lines correspond to sample G_{in}, (G_{out}). As it can be seen in this figure, there are no significant differences in the 1–halo term between the two correlation functions. Thus, the galaxy density profile of groups residing in FVS and elsewhere are remarkably similar. These results are consistent with Yaryura et al. (2012) who analysed the 2–halo term difference between groups residing in and out FVS.

3.3 Estimates of cluster sizes

It is difficult to address a reliable characteristic size of a galaxy group in observational data. The virial radius r_V, is often used to represent groups spatial extent. By definition, and assuming galaxy masses to be known, the virial radius is related to the total energy of the system through the Virial Theorem. The resulting virial radius estimate is sensitive to small separations, leading in some cases to a significant overestimation of group size.

The minimal enclosing circle is a suitable alternative estimate of group size which gives a representative measure of the group boundaries. In two dimensions, the general minimal enclosing circle problem consists of searching the smallest possible circle that encloses all the members (Sylvester 1857). Since it is a classical problem of computational geometry, several algorithms have been developed to solve it efficiently (e.g. Welzl (1991); Gärtner (1999); Mordukhovich et al. (2011)). The minimal enclosing circle has been used to define the characteristic size of galaxy systems, in particular in studies of compact groups (Hunsberger et al. 1998).

We have computed the minimal enclosing circle radii (R^{mec}) for the groups of samples G_{in} and G_{out} using the MINIBALL software (Gärtner 1999). The results are shown in figure 9. According to this figure, at a given total group luminosity, group sizes (as estimated via R^{mec}) residing in FVS are larger than those of groups

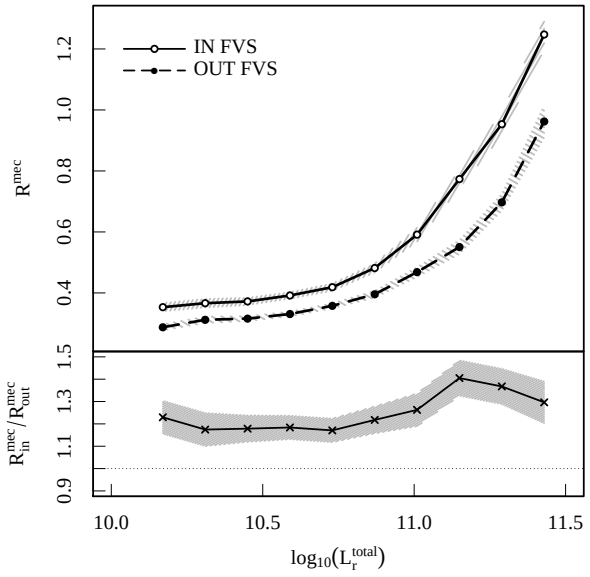

Figure 9. Upper panel: Mean radius of the minimal enclosing circle of groups, in bins of group mean luminosities, for groups in G_{in} (solid line) and G_{out} (dashed line). The error bands correspond to the error of the means. Bottom panel: ratio of the radius of the minimal enclosing circle for group samples G_{in} and G_{out}.

elsewhere. We suggest that the FoF group finding algorithm could influence this result since the neighbourhood of groups in FVS has a higher background level that may link surrounding substructures and induce larger systems.

3.4 Internal Structure of Groups

We have used the minimal enclosing circle radius defined in section 3.3 to normalize the radial distance of galaxies in a group with respect to the geometrical center, in order to analyse the stellar mass and star–formation rate profiles. We have stacked groups of samples G_{in} and G_{out} to compute mean radial profiles of the stellar mass and star–formation rate (Fig. 10).

We find that the both, the stellar mass profile and the star–formation rate of groups in samples G_{in} and G_{out} differ from each other. G_{in} systems show a larger stellar mass content and star–formation rate, and imply a larger time–scale for star formation at all distances from the group center. Figure 11 shows the mean τ parameter as a function of group–centric distance for samples G_{in} and G_{out} showing a similar behaviour althogh τ values in G_{in} are systematically larger than the G_{out} counterpart at the same group–centric distance.

4 GROUP GLOBAL PROPERTIES AND THEIR DEPENDENCE ON THE GLOBAL ENVIRONMENT

According to the current modelling of the hierarchical clustering scenario, the mass of dark matter halos is the main responsible of their properties (Bond et al. 1991; Lacey & Cole 1993; Mo & White 1996; Sheth et al. 2001). However, this assumption ignores correlations between different spatial scales, implying that the large–scale environment where the halo resides has no influence on its formation and evolution. Sheth & Tormen (2004) find evidence that haloes in dense regions form earlier than haloes of the same mass embedded in less dense regions. Using numerical N–body simulations, Gao et al. (2005) show that halos assembled at high redshift are more clustered than those of the same mass that assembled more recently. This effect, known as "assembly bias", stays that the properties of a given mass halo depend on its formation history. Hence, if galaxy clusters and groups residing in superstructures have been evolving under different environmental conditions, it is expected to find differences in their present day properties. In this context, Einasto et al. (2005) use numerical simulations to show that the density distribution in large low density regions (such as voids) present slow evolution, that cease at intermediate redshifts. On the other hand, in higher density regions (superclusters) the structures begin to form early and continue evolving until the present. Wang et al. (2008) find that SDSS galaxy groups with a red central galaxy are more strongly clustered than groups of the same mass hosting a blue central galaxy. Besides the differences on clustering amplitudes, Zapata et al. (2009) observe that galaxy groups in narrow ranges of masses but diverse formation histories present different galaxy populations. Analysis of substructure on low density regions manifest that the luminosity and local density are not completely responsible of galaxy properties. Ceccarelli et al. (2008) asset that galaxies inhabiting void walls are systematically bluer and more actively star–forming than field galaxies at a given luminosity and local galaxy density.

Since the highest density peaks, represented by superstructures, are expected to be the first sites of gravitational collapse, the assembly bias scenario can provide some light on our results. As our group samples have the same luminosity distributions (a proxy for mass distributions), differences found in their properties can be then associated to the large–scale environmental effects. In agreement with Einasto et al. (2012), we find that groups residing in superstructures are richer and present larger velocity dispersions than those in less–dense global regions. Regarding to the stellar population, the fraction of young galaxies in groups tends to be small when the systems are located on superstructures. Also, the time–scale computed from the present–day star–formation rate indicates that groups inhabiting high density regions assembled earlier than groups elsewhere. This is consistent with the previous analysis of Lietzen et al. (2012). It is expected that groups in superstructures would be the first sites of star formation in the universe and thus are likely to lack a gas reservoir suitable for present–day star formation activity.

5 CONCLUSIONS

We have adopted global luminosity, i.e. the sum of group member luminosities, as a group parameter. Using this parameter, differences in properties of groups residing in superstructures can be confronted to those elsewhere. The use of global luminosity in our work is reinforced by the fact that numerical simulations show it as a suitable proxy to group total mass (Eke et al. 2004). The main results of this work are summarized as follows:

- We find that groups residing in superstructures have a systematically larger stellar mass content exceeding by a factor 1.3 that corresponding to groups elsewhere. This relative excess of the stellar mass content is independent of group luminosity.
- The mean velocity dispersion of galaxies in groups residing in superstructures are $\sim$ 35 per cent higher than their field counterpart. The minimal enclosing radii of groups in superstructures are systematically larger by 20 per cent.

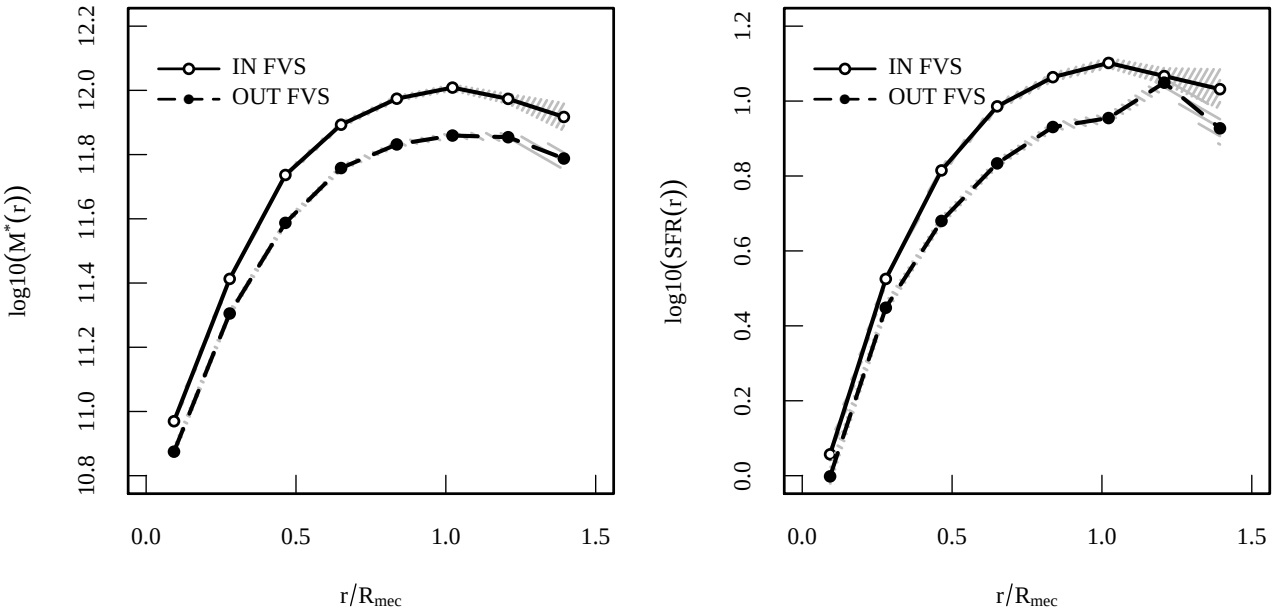

Figure 10. Group radial profiles of stellar mass (left panel) and total star–formation rates (right panel) for group samples G_{in} and G_{out}. The error bands correspond to the error of the means.

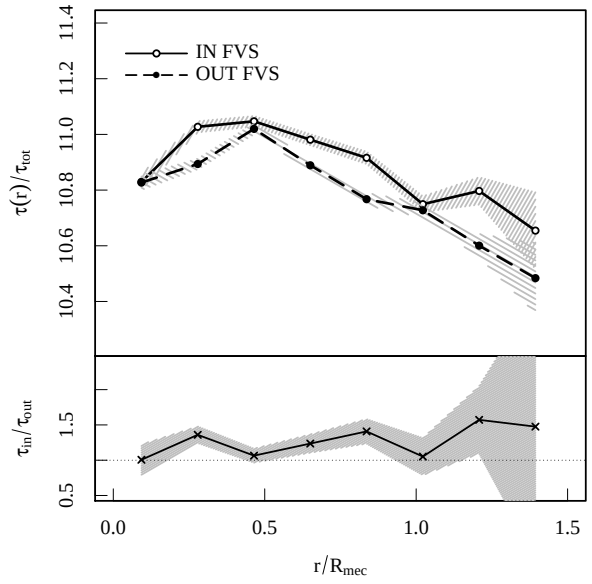

Figure 11. Group radial profile of mean stellar time–scale of group samples G_{in} and G_{out}.The error bands correspond to the error of the means. Bottom panel: ratio of the mean age for group samples G_{in} and G_{out}.

• A time–scale for star formation defined from the present–day star–formation rate shows that groups in superstructures are systematically older. Consistently, the fraction of galaxies dominated by a young stellar population, $Dn_{4000} < 1.5$, shows the same tendency.

The similarity of the star–formation rate and stellar mass group–centric radial profiles also reinforce our intrepretation in terms of the assembly bias scenario since the differences found are global. Therefore, our results provide evidence that groups in superstructures formed earlier than elswhere, as expected in the assembly bias scenario.

ACKNOWLEDGEMENTS

We thank the referee, Heidi Lietzen, for her through review and highly appreciate the comments and suggestions, which greatly improved this work. This work was partially supported by the Consejo Nacional de Investigaciones Científicas y Técnicas (CONICET), and the Secretaría de Ciencia y Tecnología, Universidad Nacional de Córdoba, Argentina. Funding for the SDSS and SDSS–II has been provided by the Alfred P. Sloan Foundation, the Participating Institutions, the National Science Foundation, the U.S. Department of Energy, the National Aeronautics and Space Administration, the Japanese Monbukagakusho, the Max Planck Society, and the Higher Education Funding Council for England. The SDSS Web Site is http://www.sdss.org/. The SDSS is managed by the Astrophysical Research Consortium for the Participating Institutions. The of the Royal Astronomical Society Participating Institutions are the American Museum of Natural History, Astrophysical Institute Potsdam, University of Basel, University of Cambridge, Case Western Reserve University, University of Chicago, Drexel University, Fermilab, the Institute for Advanced Study, the Japan Participation Group, Johns Hopkins University, the Joint Institute for Nuclear Astrophysics, the Kavli Institute for Particle Astrophysics and Cosmology, the Korean Scientist Group, the Chinese Academy of Sciences (LAMOST), Los Alamos National Laboratory, the Max-Planck-Institute for Astronomy (MPIA), the Max-Planck-Institute for Astrophysics (MPA), New Mexico State University, Ohio State University, University of Pittsburgh, University of Portsmouth, Princeton University, the United States Naval Observatory, and the University of Washington. The Millenium Run simulation used in this paper was carried out by the Virgo Supercomputing Consortium at the Computer Centre of the Max–Planck Society in

Garching. The semi–analytic galaxy catalogue is publicly available at http://www.mpa-garching.mpg.de/galform/agnpaper. Plots are made using R software.

REFERENCES

Alimi J.-M., Valls-Gabaud D., Blanchard A., 1988, A&A, 206, L11
Araya-Melo P. A., Reisenegger A., Meza A., van de Weygaert R., Dünner R., Quintana H., 2009, MNRAS, 399, 97
Binggeli B., 1982, A&A, 107, 338
Bond J. R., Cole S., Efstathiou G., Kaiser N., 1991, ApJ, 379, 440
Bond N. A., Strauss M. A., Cen R., 2010, MNRAS, 409, 156
Brinchmann J., Charlot S., White S. D. M., Tremonti C., Kauffmann G., Heckman T., Brinkmann J., 2004, MNRAS, 351, 1151
Ceccarelli L., Padilla N., Lambas D. G., 2008, MNRAS, 390, L9
Colless M., Dalton G., Maddox S., Sutherland W., Norberg P., Cole S., Bland-Hawthorn J., Bridges T., et al. 2001, MNRAS, 328, 1039
Cooray A., Sheth R., 2002, PhysRep, 372, 1
Costa-Duarte M. V., Sodré L., Durret F., 2012, MNRAS, p. 133
Crain R. A., Theuns T., Dalla Vecchia C., Eke V. R., Frenk C. S., Jenkins A., Kay S. T., Peacock J. A., Pearce F. R., Schaye J., Springel V., Thomas P. A., White S. D. M., Wiersma R. P. C., 2009, MNRAS, 399, 1773
Croft R. A. C., Matteo T. D., Khandai N., Springel V., Jana A., Gardner J. P., 2012, MNRAS, 425, 2766
de Lapparent V., Geller M. J., Huchra J. P., 1986, ApJL, 302, L1
Donoso E., O'Mill A., Lambas D. G., 2006, MNRAS, 369, 479
Dünner R., Araya P. A., Meza A., Reisenegger A., 2006, MNRAS, 366, 803
Einasto J., Einasto M., Tago E., Saar E., Hutsi G., Joeveer M., Liivamagi L., Suhhonenko I., Jaaniste J., Heinamaki P., Muller V., Knebe A., Tucker D., 2007, A&A, 462, 811
Einasto J., Tago E., Einasto M., Saar E., Suhhonenko I., Heinamaki P., Hutsi G., Tucker D., 2005, A&A, 439, 45
Einasto M., Einasto J., Muller V., Heinamaki P., Tucker D., 2003, A&A, 401, 851
Einasto M., Einasto J., Tago E., Saar E., Liivamägi L. J., Jõeveer M., Hütsi G., Heinämäki P., Müller V., Tucker D., 2007, A&A, 464, 815
Einasto M., Liivamägi L. J., Tempel E., Saar E., Vennik J., Nurmi P., Gramann M., Einasto J., Tago E., Heinämäki P., Ahvensalmi A., Martínez V. J., 2012, A&A, 542, A36
Einasto M., Suhhonenko I., Heinämäki P., Einasto J., Saar E., 2005, A&A, 436, 17
Eke V. R., Baugh C. M., Cole S., Frenk C. S., Norberg P., Peacock J. A., Baldry I. K., Bland-Hawthorn J., et al. 2004, MNRAS, 348, 866
Gao L., Springel V., White S. D. M., 2005, MNRAS, 363, L66
Gärtner B., 1999, Algorithms, ESA 99, 1643, 325
Gil-Marín H., Jimenez R., Verde L., 2011, MNRAS, 414, 1207
Gorgas J., Cardiel N., Pedraz S., 1998, Ap&SS, 263, 167
Gorgas J., Cardiel N., Pedraz S., González J. J., 1999, A&AS, 139, 29
Gregory S. A., Thompson L. A., 1978, ApJ, 222, 784
Hamilton D., 1985, ApJ, 297, 371
Hoffman Y., Lahav O., Yepes G., Dover Y., 2007, JCAP, 10, 16
Hunsberger S. D., Charlton J. C., Zaritsky D., 1998, ApJ, 505, 536
Joeveer M., Einasto J., Tago E., 1978, MNRAS, 185, 357
Kauffmann G., Heckman T. M., White S. D. M., Charlot S., Tremonti C., Brinchmann J., Bruzual G., et al. 2003, MNRAS, 341, 33
Lacey C., Cole S., 1993, MNRAS, 262, 627
Lietzen H., Tempel E., Heinämäki P., Nurmi P., Einasto M., Saar E., 2012, A&A, 545, A104
Luparello H., Lares M., Lambas D. G., Padilla N., 2011, MNRAS, 415, 964
Merchan M. E., Zandivarez A., 2005, ApJ, 630, 759
Mo H. J., White S. D. M., 1996, MNRAS, 282, 347
Mordukhovich B. S., Mau Nam N., Villalobos C., 2011, ArXiv e-prints
Park C., Choi Y.-Y., 2009, ApJ, 691, 1828
Pompei E., Iovino A., 2012, A&A, 539, A106
Ross A. J., Tojeiro R., Percival W. J., 2011, MNRAS, 413, 2078
Salim S., Rich R. M., Charlot S., Brinchmann J., Johnson B. D., Schiminovich D., Seibert M., Mallery R., Heckman T. M., Forster K., Friedman P. G., Martin D. C., Morrissey P., Neff S. G., Small T., 2007, ApJS, 173, 267
Sánchez Almeida J., Terlevich R., Terlevich E., Cid Fernandes R., Morales-Luis A. B., 2012, ApJ, 756, 163
Saunders W., Rowan-Robinson M., Lawrence A., 1992, MNRAS, 258, 134
Sheth R. K., 2005, MNRAS, 364, 796
Sheth R. K., Mo H. J., Tormen G., 2001, MNRAS, 323, 1
Sheth R. K., Tormen G., 2004, MNRAS, 350, 1385
Strauss M. A., Weinberg D. H., Lupton R. H., Narayanan V. K., Annis J., Bernardi M., Blanton M., Burles S., Connolly A. J., Dalcanton J., Doi M., Eisenstein D., et al. 2002, AJ, 124, 1810
Swanson M. E. C., Tegmark M., Blanton M., Zehavi I., 2008, MNRAS, 385, 1635
Sylvester J. J., 1857, Quarterly Journal of Pure and Applied Mathematics, 1, 79
Tempel E., Einasto J., Einasto M., Saar E., Tago E., 2009, A&A, 495, 37
Wang W., Jing Y. P., Li C., Okumura T., Han J., 2011, ApJ, 734, 88
Wang Y., Yang X., Mo H. J., van den Bosch F. C., Weinmann S. M., Chu Y., 2008, ApJ, 687, 919
Welzl E., 1991, New results and new trends in computer science, 555, 539
White M., Cohn J. D., Smit R., 2010, MNRAS, 408, 1818
Yaryura C. Y., Lares M., Luparello H. E., Paz D. J., Lambas D. G., Padilla N., Sgró M. A., 2012, MNRAS, 426, 708
York D. G., Adelman J., Anderson Jr. J. E., Yanny B., Yasuda N., 2000, AJ, 120, 1579
Zapata T., Perez J., Padilla N., Tissera P., 2009, MNRAS, 394, 2229
Zehavi I., Weinberg D. H., Zheng Z., Berlind A. A., Frieman J. A., Scoccimarro R., Sheth R. K., Blanton M. R., Tegmark M., Mo H. J., Bahcall N. A., Brinkmann J., Burles S., Csabai I., Fukugita M. a., 2004, ApJ, 608, 16
Zehavi I., Zheng Z., Weinberg D. H., Blanton M. R., Bahcall N. A., Berlind A. A., Brinkmann J., Frieman J. A., Gunn J. E., Lupton R. H., Nichol R. C., 2011, ApJ, 736, 59
Zehavi I., Zheng Z., Weinberg D. H., Frieman J. A., Berlind A. A., Blanton M. R., Scoccimarro R., York D. G., 2005, ApJ, 630, 1
Zeldovich I. B., Einasto J., Shandarin S. F., 1982, Nature, 300, 407